Journal of Membrane Science 620 (2021) 117712

Contents lists available at ScienceDirect

Journal of Membrane Science

journal homepage: http://www.elsevier.com/locate/memsci

Fabrication of self-doped sulfonated polyaniline membranes with enhanced antifouling ability and improved solvent resistance

Ida Francesca Amura [a,b], Salman Shahid [a,b,**], Adem Sarihan [c], Junjie Shen [a,b], Darrell Alec Patterson [a,b], Emma Anna Carolina Emanuelsson [a,*]

[a] Department of Chemical Engineering, University of Bath, Bath, BA2 7AY, United Kingdom
[b] Centre for Advanced Separations Engineering, University of Bath, Bath, BA2 7AY, United Kingdom
[c] Bilecik Vocational School, Bilecik Seyh Edebali University, Bilecik, 11230, Turkey

ARTICLE INFO

Keywords:
Low fouling
Self-doped polyaniline
Solvent resistance
Chemical cross-linking
Tight UF membranes

ABSTRACT

The fabrication of self-doped sulfonated polyaniline S-PANI membranes is reported here for the first time and addresses key challenges of PANI membranes including fouling, solvent stability issues and acid leaching. Sulfonation of the PANI-powder was confirmed by FTIR, UV-VIS and SEM-EDX characterisation. The membranes were prepared via phase inversion approach in water from a solution of 23% w/v S-PANI and were chemically cross-linked with three different organic cross-linkers: α,α′-Dichloro-p-xylene (DCX), glutaraldehyde (GA) and terephtaloyl chloride (TCL). PANI, S-PANI, S-PANI DCX, S-PANI TCL and S-PANI-GA were evaluated for their hydrophilicity, morphology, chemical properties and filtration performance showing that the chemically cross-linked S-PANI membranes have superior stability and reusability in DMF when tested in dead-end cell at 5 bar. Filtration experiments in water showed that S-PANI-GA has an increase in PEG rejection of 2.3 times and a MWCO of 1800 Da in contrast with PANI and SPANI, which showed a MWCO above 5000 Da. Fouling performance using BSA, showed a significant improvement of flux recovery for S-PANI and S-PANI GA, with the membranes regaining 87% and 83% of their original flux after one cleaning-fouling cycle. Conversely, PANI had a flux recovery of only 40%. The low irreversible fouling of the membranes, 13% for S-PANI and 17% for S-PANI GA, against 65% for PANI after 3 cycles is an encouraging result for the reduction of costly and high environmentally impact chemical cleaning in membrane processes. Overall, this study provides a simple method to produce low fouling and long-term solvent resistant membranes to enhance the widespread use of membrane technology in industrial processes.

1. Introduction

The significant advantages of polymer membranes are that their properties can be easily modified for a wide range of applications through synthesis, the availability of many natural and synthetic polymers and cheaper cost compared to ceramic materials [1]. Despite the significant progress in membrane technology, there are still challenges to overcome namely: (i) high tendency to fouling [2,3] (chemical and physical cleaning only partially recover the membrane performance [4–6]) and (ii) solvent stability in the low UF/NF range.

Much research has focussed on modifying pre-formed membranes (i.e. post-modification) to make them more hydrophilic (thus high-fouling resistant) by, for example, co-addition of hydrophilic polymers and zwitterionic materials using chemical/physical methods. Chemical modification mainly involves grafting, plasma and UV treatment [7,8], whereas physical methods involve coating and blending with hydrophilic polymers [5,9]. These methods have shown limited success in modifying the antifouling behaviour of the membranes (see reviews by Rana et al. [3] and Nady et al. [10]), thus calling for more straightforward and cheaper methods. Recently, S-PANI has been investigated as an additive to produce low-fouling membranes for water applications [5,11,12]. S-PANI is part of the PANI family, a widely used conducting polymer for membrane fabrication because of its environmental stability, low cost and its interesting redox chemistry [13–15]. In S-PANI, SO_3H is covalently bonded to the benzene rings, resulting in a permanent hydrophilic modification and doping of the system [16,17]. The

* Corresponding author.
** Corresponding author. Department of Chemical Engineering, University of Bath, Bath, BA2 7AY, United Kingdom.
E-mail addresses: s.shahid@bath.ac.uk (S. Shahid), eaep20@bath.ac.uk (E.A.C. Emanuelsson).

https://doi.org/10.1016/j.memsci.2019.117712
Received 26 June 2019; Received in revised form 31 October 2019; Accepted 30 November 2019
Available online 2 December 2019
0376-7388/

polymer was firstly reported in 1990 [18] and since then it has been used for various application such as batteries, H_2O_2 sensors, synthesis of nanofibers and hydrogels [19–22].

In membrane fabrication, the preparation of composite membranes consists of a multi-step procedure where i) PANI is synthesised via chemical polymerization and ii) the sulfonation step occurs [5,11,12]. However, because of its self-doped nature, it readily forms a gel-like structure, making it hard to form a membrane. The polymer is de-doped and blended with other hydrophobic polymers before casting. Hence, as the fabrication of pure S-PANI membrane has never been attempted before, we suggest to co-polymerise aniline and metanilic acid [23], as a straightforward method to synthesise S-PANI and then prepare the membrane via non-solvent phase inversion.

The aim of this research is to develop a new family of membranes using pure S-PANI. We have therefore synthesised a low fouling S-PANI membrane via non-solvent phase inversion and compared its morphology, performance and antifouling properties with PANI membrane. To further improve the solvent resistance of the S-PANI membrane, the effect of DCX and GA as chemical cross-linkers (previously used to prepare nanofiltration PANI membrane [24]) will be investigated. Furthermore, we will report for the first time the effect of TCL in cross-linking self-doped S-PANI. Permeance and rejection of the developed S-PANI membranes were measured in a dead-end cell using pure water and a solution of different molecular weight polyethylene glycols. Solvent stability was tested in a range of solvents in both static (immersion test) and dynamic mode (in-filtration test). The low fouling behaviour of S-PANI membranes was evaluated in a cross-flow cell using BSA as model foulant.

2. Experimental methods

2.1. Materials

Aniline, ammonium persulfate (APS), hydrochloric acid (HCl), HPLC grade acetone, DMF, DMAc, Toluene, N-methyl-2-pyrrolidone (NMP) and 4-methyl piperidine (4-MP) were purchased from Sigma-Aldrich (UK) along with the chemical cross linkers α,α′-Dichloro-p-xylene (DCX), glutaraldehyde (GA) and terephtaloyl chloride (TCL). Commercial grade polyethylene glycols (PEGs of molecular weight 1000, 1500, 4000 and 6000), ethanol, methanol, and isopropanol were obtained from Fisher (UK). PET/PBT backing layer- Novatexx 2484 (120 μm) was supplied by Freudenberg Filter technologies (Germany). All solutions were prepared with deionised (DI) water produced from an ELGA deioniser (PURELAB Option).

2.2. Synthesis of sulfonated polyaniline (S-PANI) and polyaniline (PANI)

S-PANI was synthesised by radical polymerization of aniline and metanilic acid in the presence of ammonium persulfate in acidic medium as shown in Fig. 1. This synthetic route is reported to produce more thermally stable S-PANI [23]. In a 1 L beaker in an ice bath were dissolved 0.05 mol of metanilic acid and 0.05 mol of ammonium persulfate in 800 ml of HCl 0.1 M, and the mixture was stirred. After 5 min 0.05 mol of aniline was added dropwise in 1 h. The reaction was allowed to stir for 6 h and then decanted all night to allow precipitation of the polymer. The reaction mixture was washed exhaustively with water and then acetone until neutral pH of the washing solution was reached. The resulting green product was dried in vacuum oven at 50 °C for 24 h. The product was analysed via infrared (FT-IR) spectroscopy and UV-VIS spectroscopy, and the sulfur: nitrogen ratio was confirmed by SEM-EDX.

2.3. Membrane fabrication

Table 1 summarises the optimisation study performed to select the concentration of polymer and composition of the dope solution.

S-PANI powder was slowly added to the mixture of solvent and additives using a funnel in small portions over 5 min. The mixture was stirred at a low mixing speed (50–70 rpm) for 12 h to obtain a homogeneous solution and then left overnight to remove air bubbles. PANI was instead prepared adding 1.5 g of powder (20 wt %) to a mixture of NMP (5.5 g) and 4-MP (0.5 g). The mixture was stirred for 12 h and then left overnight to remove air bubbles.

The membranes were prepared via phase inversion method at room temperature. DI water was used as the non-solvent in the coagulation bath.

All membranes were cast on a benchtop laboratory caster. The Novatexx 2484 membrane backing layer was secured using scotch tape on a flat glass plate. An adjustable casting knife was used to cast the film using an adjustable film applicator (Elcometer 4340 automatic film applicator, Elcometer, UK). Evaporation time of 30 s was used before immersing the casted membrane solution into a DI water coagulation bath. The membrane was kept immersed in DI water at room temperature for at least 24 hs and then rinsed with fresh water and stored in DI water for later chemical and thermal treatments.

2.3.1. Chemical cross-linking reactions with DCX, TCL and GA

Chemical cross-linking of S-PANI membranes took place at 20 °C and was performed as follow: A cross-linking solution of 0.2 M DCX in acetone/hexane (35/65 v/v%) mixture was used and the membranes were cross-linked following a procedure previously reported [24]. The membranes were kept in the cross-linker solution for 3 days and after cross-linking were washed 2 times with acetone and stored in water for future use.

S-PANI membranes were cross-linked in a 0.1 M solution of TCL in THF at room temperature for the desired amount of time (48 h). Fig. 2 reports the cross-linking of S-PANI with TCL, which occurs in the amine nitrogen of the polymer. Membranes were then washed 3 times with THF and stored in water/isopropanol for future use.

After casting, S-PANI membranes were kept immersed in 600 ml of a

Table 1
Screening of thickness, concentration, and composition for the preparation of S-PANI membranes.

Membrane (notation)	Thickness (μm)	S-PANI wt.%	dope solution
MSP15	200	15	NMP/4-MP
MSP18	200	18	NMP/4-MP
MSP18T	200	18	NMP/4-MP/THF
MSP20	200	20	NMP/4-MP
SPWT01	250	20	NMP/4-MP
MSP23	200	23	NMP/4-MP/THF

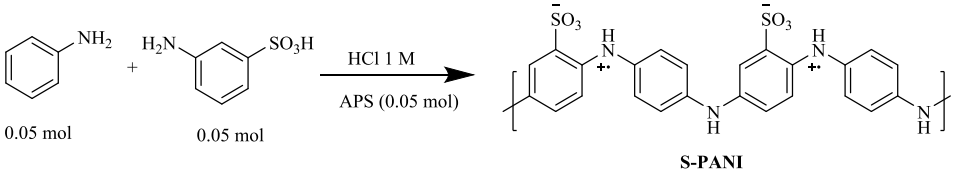

Fig. 1. Radical polymerization of aniline and metanilic acid mediated by APS in HCl. Polyaniline was synthesised using a method reported elsewhere [14].

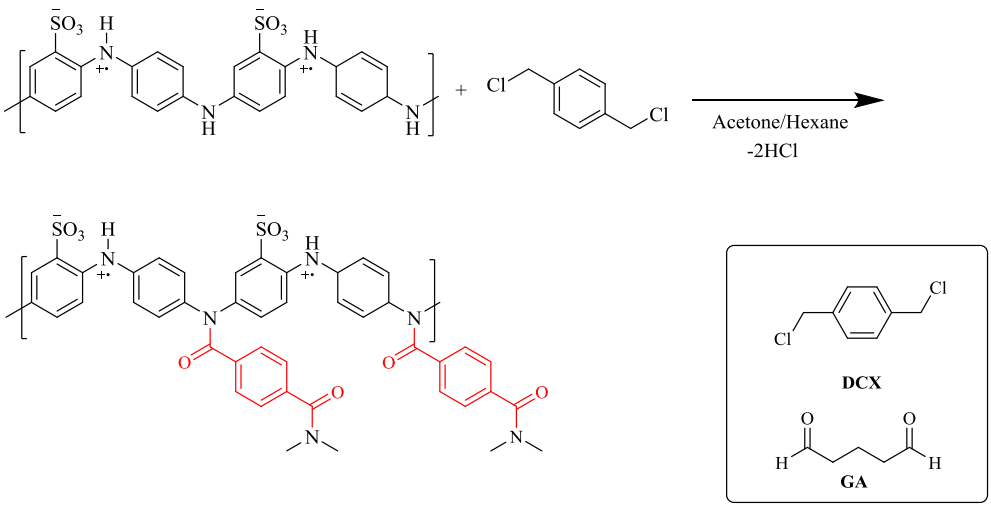

Fig. 2. Example of a reaction scheme for the chemical cross-linking of S-PANI with TCL. Chemical cross-linking with DCX and GA is reported for PANI here [24].

cross-linker solution containing 50 ml of GA (50 wt% solution) and 50 ml of HCL (12 M) in water for phase inversion. A glass box equipped with a lid was used to contain the crosslinking solution. After 1 h, 400 ml of acetone was added to the membranes and the box was sealed and left for 5 days until reaction completion. After cross-linking membranes were stored in water.

2.4. Characterization techniques

The FTIR spectra of dry S-PANI samples (both powder and membranes) and PANI powder were obtained by using a Spectrum 100™ – FTIR Spectrometer (PerkinElmer, USA) fitted with an attenuated total reflectance (ATR) detector. A background scan was run prior to sample testing and spectra were recorded from 4000 to 650 cm^{-1} in transmission mode with a spectral resolution of 4 cm^{-1} and 32 scans.

S-PANI and PANI powders were analysed by UV–vis spectrometry (UV-1601, Shimadzu, Japan). 100 mg of powder was dissolved in 100 mL of NMP to prepare 1.0 g/L solution; the obtained solution was then diluted to 1.0 × 10^{-2} g L^{-1} by NMP. Spectra were recorded at wavelengths from 250 to 850 nm at room temperature.

Membrane morphology was studied using FSEM (JSM-6301F, JEOL, Germany). All samples were prepared by freeze fracturing them in liquid nitrogen and drying them in vacuum overnight. Before the analysis was performed the samples were coated in chromium using a sputter coater (Q150T S, Quorum) under argon for 5 min.

Membrane hydrophilicity was studied by dynamic contact angle analysis. (Contact Angle System OCA 15Pro, Dataphysics, Germany). The analysis was performed using the sessile drop technique (4 μL) and data were recorded for 800 s and repeated 2 times.

X-ray diffractometry XRD was used to characterise the pure S-PANI membrane and the cross-linked membranes. XRD spectra were scanned on a STOE STADI P double setup, equipped with mythen detectors, using pure Cu-Kα1 radiation (λ = 1.54060 Å).

2.5. Evaluation of membrane performance

2.5.1. Dead-end filtration

A dead-end cell (HP 4750, Sterlitech, USA) was employed to measure solvent permeance and solute rejections of the pure S-PANI membranes and the chemical cross-linked S-PANI membranes. A PEG solution was used to determine membrane solute permeance and rejection in water and using the following concentrations: PEG 1000 (600 ppm) PEG 3000 (2400 ppm), PEG 4000 (2400 ppm) and PEG 6000 (2400 ppm. During all the filtration tests a pre-conditioning step was performed for the permeate flux to reach steady state. Pure water flux is defined as follows:

$$Jw = \frac{V}{A \times \Delta t} \quad (1)$$

Where V (L) is the permeate volume; A (m^2) is the membrane effective filtration area and Δt (h) is the filtration time. The PEGs concentrations were analysed using an HPLC apparatus (Agilent 1260 infinity series, Agilent Corporation, USA) consisted of an autosampler (G1329B) coupled with an ELSD detector A flowrate of 1.0 mL min^{-1} was used with mobile phase acetonitrile/water (15/85). The peaks in the chromatogram were analysed using an already established method [25,26]. PEGs rejection was calculated by following Eq. (2) where C_p and C_0 are the concentration of the solute in the permeate and in the feed, respectively.

$$R\% = \left(1 - \frac{C_p}{C_0}\right) \times 100 \quad (2)$$

2.5.2. Fouling study using BSA

The flux of S-PANI membranes was measured using a cross-flow rig which consisted of a pump, a solution bottle and a membrane cell with an effective filtration area of 14.6 cm^2. Bovine Serum Albumin BSA (1 g/L) was used to perform fouling experiments. The membranes were first pre-compacted at 2 bar with deionised water for 1 h and then the permeance was measured at 1 bar. The permeation flux of the foulant solution was calculated as Jp (L/m^2h) and a UV–Vis spectrometer (UV-1601, Shimadzu, Japan) was used to analyse the permeate samples at 278 nm. After filtration of the BSA solution, the tested membranes were extensively washed with water using the same condition of the experiment (1 bar, 0.5 L/min) and the pure water flux (Jw1, L/m^2h) of the cleaned samples was measured again. In order to measure the fouling resistance ability of the synthesised S-PANI and cross-linked SPANI membranes, fouling indexes were calculated using the following equations:

$$FRR\ \% = \frac{Jw1}{Jw} \times 100 \quad (3)$$

$$TFR\ \% = \left(1 - \frac{Jp}{Jw}\right) \times 100 \quad (4)$$

$$RFR\ \% = \left(\frac{Jw1 - Jp}{Jw}\right) \times 100 \quad (5)$$

$$IFR\ \% = \left(1 - \frac{Jw1}{Jw}\right) \times 100 \quad (6)$$

Where FRR is the water flux recovery ratio, TFR is the total fouling ratio, RFR is reversible fouling ratio and IFR is the irreversible fouling ratio. Membranes with a high value of FRR and a low IFR have better anti-fouling properties [6]. The flux recovery ratio of the membrane after 3 cycles (Fr) was calculated as follow:

$$Fr\,\% = \left(\frac{J}{J_0}\right) \times 100 \quad (7)$$

Where J_0 is the initial pure water flux of the membrane before any fouling occurs.

3. Results and discussion

3.1. Characterization of S-PANI powder

FT-IR confirmed the chemical structure of S-PANI and PANI membranes (Fig. 3 (A)). The PANI spectrum has two characteristic peaks at 1449 cm^{-1} and 1554 cm^{-1} corresponding to the benzenoid and quinoid form of PANI. The band at 1279 cm^{-1} can be assigned to both C–H and C–N stretches whereas the para-disubstitution characteristic of PANI can be reflected by the peak at 810 cm^{-1} of the C–H bending out of plane [27]. The FT-IR spectrum of S-PANI has additional peaks at ~1030-1070 cm^{-1} (S═O stretching) and another at 707 cm^{-1} (S–O stretching). The peak at 825 cm^{-1} can be assigned to the tri-substitution of the benzene ring. Characterization results are in agreement with the literature [5].

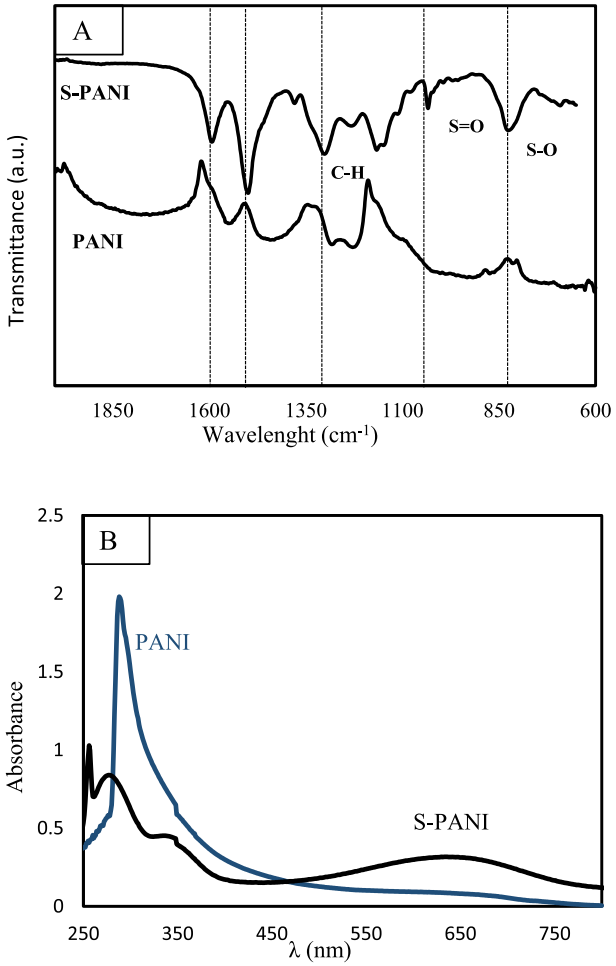

Fig. 3. (A) Comparison of FTIR spectra of S-PANI and PANI membranes to confirm sulfonation, (B) UV-VIS spectra of PANI powder and S-PANI powder in NMP (0.01 g/L).

UV-VIS spectroscopy was used to observe and compare the optical properties of PANI and S-PANI. Fig. 3 (B) shows the resulting absorbance spectra of the two polymers in NMP. S-PANI has two humps at 342 nm and at 655 nm which correspond to the B-Band and the Q-band respectively. The hump at 342 nm (B-Band) derives from the π→π* transition associated with π electrons of benzenoid rings whereas the absorption in the visible range at 655 nm (Q-band) is due to the excitation of an electron from the highest occupied orbital of benzenoid rings to the lowest occupied orbital of the quinoid ring. PANI presents a shift of the same B-Band at 355 nm and the Q band is shifted at 630 nm. As reported in the literature, these results suggest that PANI has less electronic delocalization on the benzene ring because of the absence of $–SO_3H$ and that, instead these functional groups cause a self –doping effect on the quinone structure [6].

SEM-EDX analysis was used to determine the degree of sulfonation of the S-PANI powder. Both PANI and S-PANI are conducting polymers that can be converted from insulators to conductors through acid doping. PANI oxidation state can be controlled by external protonic doping, however, in S-PANI, the addition of sulfonic groups on its benzenic structure introduce a covalently bond acid group that make the polymer self-protonated or self-doped [16]. The calculated S: N ratio for the synthesised S-PANI is 0.45 corresponding to a fully doped S-PANI with both positive and negative charges [5] (see supporting info). In this oxidation state, S-PANI act as a zwitterionic polymer with high hydrophilicity and low fouling tendency [11].

3.2. Optimisation of membrane fabrication conditions and cross-linking

Table 1 reports the different parameters investigated in the preparation of S-PANI membranes. After an initial screening of polymer concentration, membrane thickness, and composition of the dope solution a 23% w/w load of polymer concentration in a mixture of NMP/4-MP and THF was selected as an optimised polymer concentration. MSP15, MSP18 and MSP1T were unstable and disintegrated when cut in coupons for filtration experiments, most likely because of weak interaction with the support layer. MSP23 was prepared from a mixture of NMP, 4-MP, and THF and was chosen as the best membrane and from now on referred only as S-PANI membrane.

Thermal cross-linking of the S-PANI membrane was investigated at different temperatures (supporting info). The exposure to the high temperatures made the membrane brittle and reduced membrane mechanical properties and filtration stability, making it non-practical for filtration studies. Therefore, this work focuses on the chemical cross-linking of S-PANI membranes rather than thermal cross-linking.

3.3. Membrane characterization

FT-IR analysis shows a comparison between the cross-linked S-PANI with pure S-PANI membrane (Fig. 4). There is no significant difference between the S-PANI membranes cross-linked with DCX, TCL and GA due to the overlapping of those bands with the S-PANI ones. The spectra of S-PANI TCL has, however, two additional peaks at 1600 cm^{-1} (amide C═O stretching) and 1200 cm^{-1} (C–N stretching for tertiary amide) that confirms the cross-linking reaction [28]. Solvent stability tests (section 3.4) indicate that chemical crosslinking has occurred.

XRD method is used to analyse the S-PANI membrane and the cross-linked membranes (Fig. 5). Polyaniline and its derivatives are semi-crystalline in nature and the x-ray diffractograms of the membranes show three characteristic peaks associated with the degree of orientation of the polymer chains in a particular crystal plane [29,30]. The cross-linked membranes show three similar peaks with different intensities, indicate a consistent orientation of the crystalline domains in the same direction as the pure S-PANI. This suggests that cross-linking does not significantly affect the crystal structure of the polymer. The

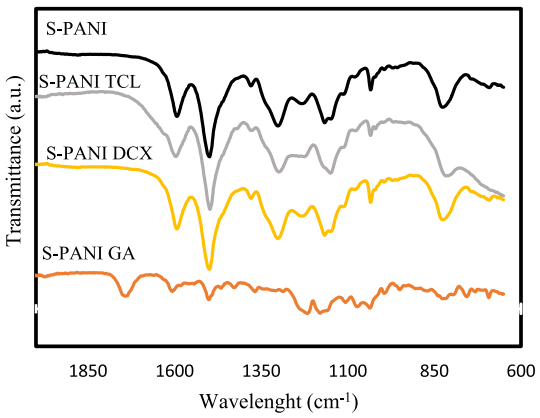

Fig. 4. Comparison of FTIR spectra of S-PANI, S-PANI GA, S-PANI DCX and S-PANI TCL membranes after cross-linking.

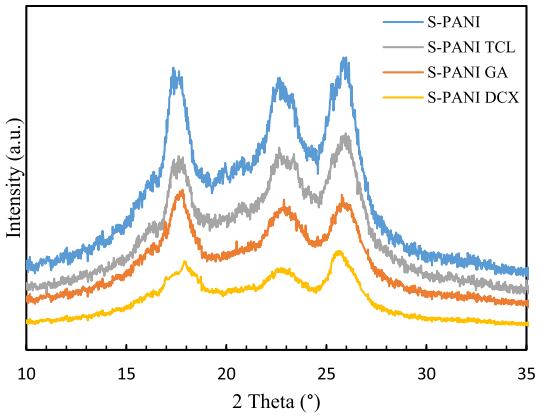

Fig. 5. XRD patterns of pure S-PANI membrane and S-PANI membranes cross-linked with GA, TCL and DCX.

cross-linked membranes show a decrease in intensity or broadening of the peak of S-PANI at $2\Theta = 22.2°$ compared to pure S-PANI. This decrease in intensity suggests that the cross-linking of S-PANI membranes led to the disordering of S-PANI crystal structure which could be attributed to shrinkage of intersegmental or d-spacing [31].

SEM was used to study the morphology of S-PANI and chemically cross-linked S-PANI membranes and compare them with pure PANI. Fig. 6 displays the top surfaces and cross-sections of all prepared membranes. All membranes show a smooth surface with no apparent pores or patterns. The small particles present on all the top surfaces are most likely impurities deriving from the sample preparation process. All cross-sections present an asymmetric structure with a porous bottom layer and a denser top skin layer. Cross-sections of PANI (Fig. 6A) and S-PANI membranes (Fig. 6B) differ with the number and size of the macro-voids and cavities; PANI has a porous layer with regular small cavities on the top and bigger voids on the bottom and S-PANI presents big and dispersed macro-voids. The morphology of S-PANI membrane is in agreement with other studies where the inclusion of the hydrophilic moiety increased the water diffusion rate during phase inversion and caused the formation of large macro-voids [4,32]. The S-PANI GA membrane (Fig. 6C) has a narrower bottom finger-like structure indifference to the other cross-linked membranes (Fig. 6D and E) that presents large voids and cavities. This difference in the structure can be attributed to the inclusion of the cross-linker solution in the coagulation bath, causing a delayed demixing [33] (see section 2.3 for the method). The macro voids present in the studied PANI, S-PANI, S-PANI TCL and S-PANI DCX membranes can be related to the better affinity between NMP used in the casting solution and water, which caused the instantaneous demixing [14]. Cross-sections of S-PANI DCX and S-PANI TCL (Fig. 6D and E) show that the former has a porous sublayer with a regular pattern of large cavities and the latter is in contrast denser with a few dispersed cavities.

3.4. Chemical cross-linking: Visual stability study in organic solvents

Stability in organic solvents was evaluated using an immersion test in different solvents. Fig. 8 shows the effect of DMF and DMAc on membranes stability.

S-PANI is directly dissolved in DMF and DMAc, giving a vivid blue solution, whereas S-PANI GA, S-PANI DCX and S-PANI TCL appear to be more resistant to the harsh polar aprotic solvents giving a slightly darker solution after 10 min. Therefore, the dissolution of the membrane was quantified through solvent resistant tests [34] to determine the effect of cross-linking on S-PANI membranes. Table 2 reports the % weight loss for each membrane after soaking the samples for 1 month in DMAc, DMF, EtOH, toluene, ethyl acetate and acetone. The test in different solvents confirms the superior chemical stability of S-PANI GA, S-PANI DCX and S-PANI TCL. The improved solvent stability is due to the formation of interchain bonds in the polymer that 1) change the physical network by creating fix points and 2) limit the molecular chain movements making the whole membrane less prone to dissolve.

These results show that S-PANI can be chemically cross-linked to prepare high solvent stable membranes for applications where chemical stable membranes are required but their availability is limited [35].

3.5. Membrane surface hydrophilicity

To assess the surface hydrophilicity, the wettability of the prepared S-PANI membranes was investigated via sessile drop technique and compared with the wettability of PANI membrane. Figs. 9 and 10 show the change in contact angle as a function of time for PANI and S-PANI, and the chemically cross-linked S-PANI membranes. PANI and S-PANI present an initial contact angle of $73 \pm 10°$ and $73 \pm 2°$ respectively. For S-PANI, the contact angles rapidly decrease reaching a value of $42 \pm 6°$ after 600 s, whereas PANI exhibits a contact angle of 61 ± 8. The higher reducing rate and therefore the lower contact of S-PANI can be attributed to a membrane with a low surface energy and good hydrophilicity. The sulfonation improves the wettability of the membranes suggesting that S-PANI could be potentially used as anti-fouling material and prevent the adhesion of organic matters on the membrane.

The cross-linked membranes present initial contact angles of $71 \pm 4°$ (S-PANI DCX), $70 \pm 7°$ (S-PANI GA) and $70 \pm 3°$ (S-PANI TCL). The overall trend for all membranes is a very small decrease in the contact angles after 600 s meaning that the cross-linking increased the H_2O transport resistance and slower the reducing rate over time. The trend for all cross-linked membrane is similar to that of pure PANI membrane. This suggests that the main factor affecting the wettability of cross-linked membranes is the slower penetration of the water drop because of the tighter pore size rather than the presence of the sulfonic group.

3.6. Filtration properties and fouling behaviour

3.6.1. Water flux and PEG rejection in water

Fig. 11 shows the pure water flux decline for all membranes at 2 bar. At least 1 h was required, for all membranes to reach a steady flux. Compaction of polymeric membranes and consequent flux decline is a well-known issue in pressure-driven processes [36]. It can further be observed that PANI shows a higher flux decline and less resistance to compaction in comparison to S-PANI. S-PANI has a stable pure water flux of 117 ± 20 L $m^{-2}h^{-1}$ and PANI has a water flux of 165 ± 35 L $m^{-2}h^{-1}$. These values are an agreement with the literature [5] and can be placed in the ultrafiltration range.

For the cross-linked membranes, S-PANI GA and S-PANI TCL show the greatest flux decline reaching values of 22 ± 8 L $m^{-2}h^{-1}$ and 13 ± 4

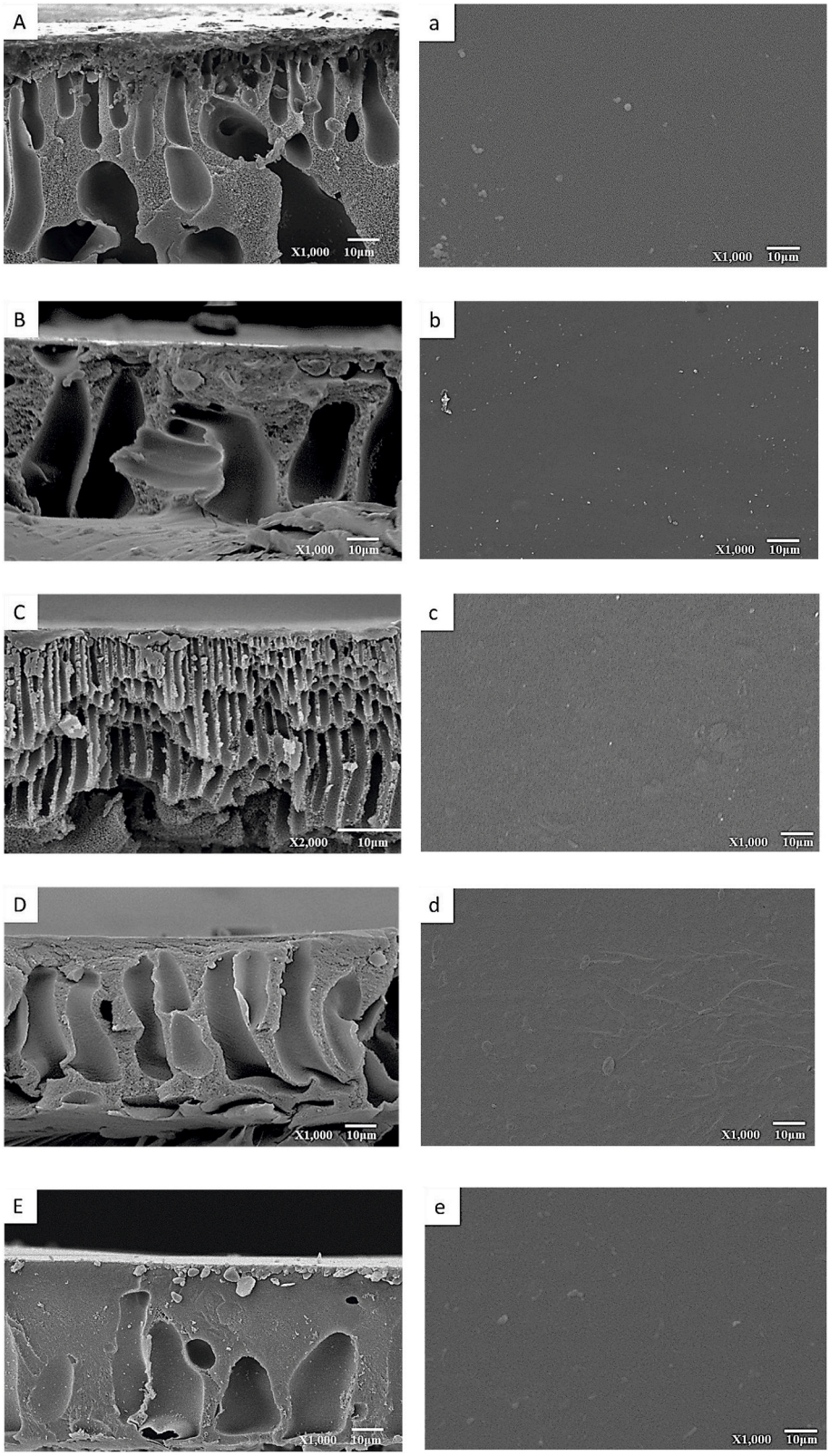

Fig. 6. Cross-section SEM images of (A) PANI (B) S-PANI (C) S-PANI GA (D) S-PANI DCX and (E) S-PANI TCL. Top Surface SEM images of PANI (a)-S-PANI (b), S-PANI GA (c), S-PANI DCX (d) and S-PANI TCL (e). Fig. 7 shows cross-sectional images of the top surface layer of the S-PANI and chemically cross-linked S-PANI membranes taken at higher magnification. The top layer of (A, a) S-PANI, (C, c) S-PANI DCX and (D, d) S-PANI TCL consists of a layer of densely packed irregular nodular structures. These nodular structures aggregate and become more porous and irregularly distributed along the bulk in the pure S-PANI membranes. In difference, they remain densely packed in the cross-linked membranes. A magnification of 10,000x and 50,000x was necessary to study the top layer of S-PANI GA membrane (B,b) which consists of spherical structures that rearrange in narrow-finger like voids.

L $m^{-2}h^{-1}$ respectively, which can be considered in the range of tight ultrafiltration. S-PANI DCX has an initial lower flux and the flux decrease below 1 ± 0.5 L m^{-2} h^{-1}. As reported in section 3.5, chemically cross-linked membranes showed a lower surface free energy and therefore a higher H_2O transport resistance that is reflected in the flux decline to very low values.

Fig. 12 shows the performance curves of S-PANI membranes and chemically cross-linked S-PANI membranes tested with different PEGs in dead-end cells. S-PANI reject only 12% for the oligomer with the highest molecular weight (PEG 5000) at 2 bar. The membrane was tested at a different pressure to evaluate its stability to elevated pressure resulting in 3 bar maximum operational conditions. This suggests that S-PANI

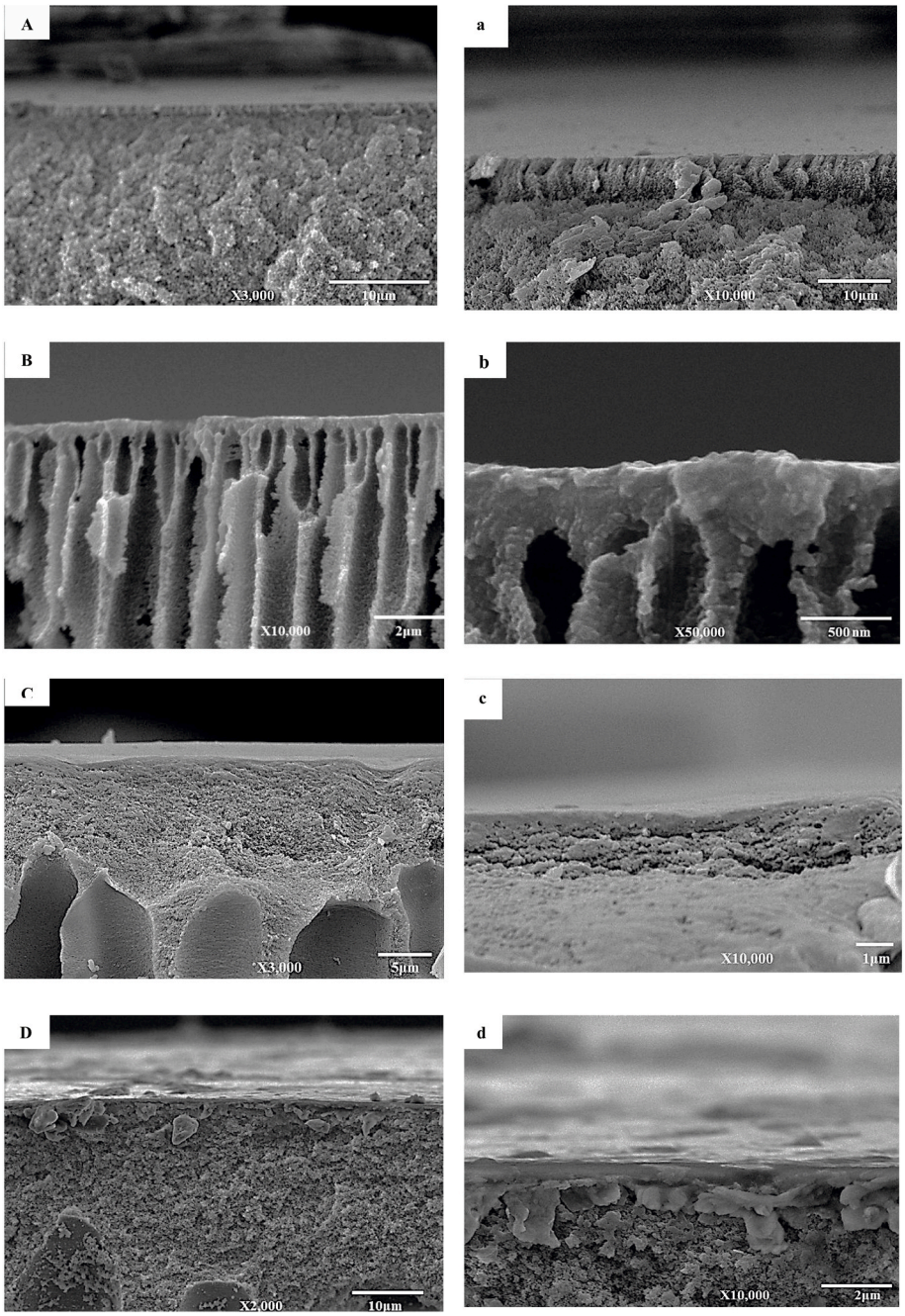

Fig. 7. Cross-section SEM images of the top surface layer of (A) S-PANI (B) S-PANI GA (C) S-PANI DCX and (D) S-PANI TCL.

membranes are suitable for the application in the UF/tight UF range, similarly to PANI membranes [37]. The addition of the sulfonic groups is a chemical modification that affects the hydrophilic properties, but has limited effect on the membrane pore size.

In comparison, the cross-linked membranes, S-PANI DCX and S-PANI TCL, were able to reject the higher MW PEG (5000 Da) of 56 and 48% respectively. These membranes showed an improve filtration stability with maximum operating pressures of 10 bar. S-PANI GA showed the best performance with a 93% rejection of the PEG 5000 and a maximum operating pressure of 30 bar. In addition, the MWCO for this membrane was found to be 1800 and S-PANI GA was the only membrane that could be fully characterised in terms of MWCO. Crosslinking forms stable bonds among the polymer chains, which allows them to be efficiently packed and overcome their high free volume and rigidity. Recent examples of chemical cross-linking of PANI with DCX and GA [24] and aniline with TCL [28,38] have been reported. In the case of PANI, chemical modification produces a nanofiltration membrane with high solvent resistance. In contrast, the results from this work show that S-PANI DCX and S-PANI TCL has an improved solvent resistance but most likely presents potential applications in the tight UF range. However, the cross-linking with GA successfully produced a membrane with a tighter pore size and almost 90% rejection of all tested PEGS. Nevertheless, all the chemically cross-linked membranes showed enhanced stability in several solvents, especially harsh polar aprotic solvents such as DMF, with respect to S-PANI. Overall, the chemical treatment makes the membrane more stable in solvents due to the formation of strong covalent bonds, but the big sulfonic groups prevent the shrinking of the membrane pore size.

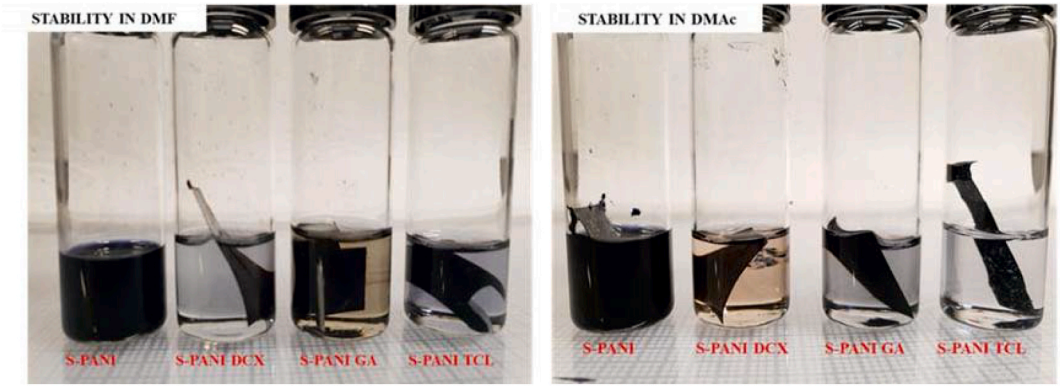

Fig. 8. Effect of DMF and DMAc on membrane stability. Picture is taken after half an hour from immersion in solvents.

Table 2
% Weight loss data for S-PANI membranes and S-PANI GA, S-PANI TCL and S-PANI DCX membranes in different organic solvents. Data were collected after 1 month of soaking in the chosen solvent.

Membrane	Weight loss in solvent					
	DMAc	DMF	EtOH	Toluene	EA	Acetone
S-PANI	11.0%	15.0%	0.0%	0.0%	0.0%	0.0%
S-PANI GA	0.40%	0.58%	0.0%	0.0%	0.0%	0.0%
S-PANI DCX	0.60%	0.47%	0.0%	0.0%	0.0%	0.0%
S-PANI TCL	0.38%	0.88%	0.0%	0.0%	0.0%	0.0%

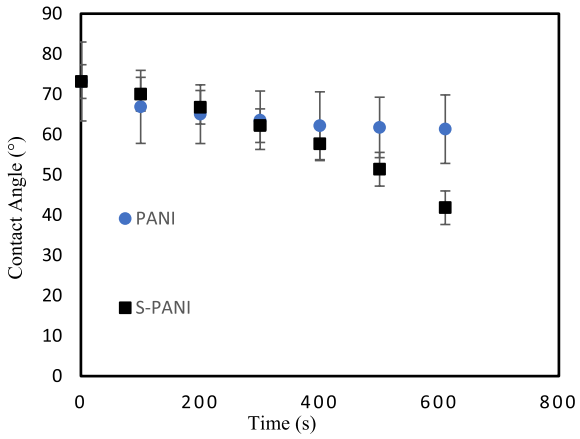

Fig. 9. Contact angles as a function of time for PANI and S-PANI membranes.

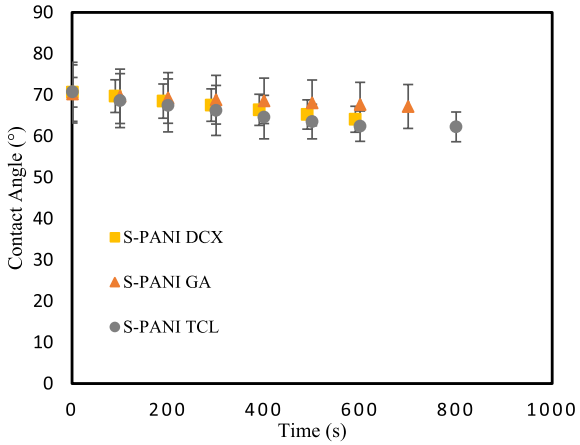

Fig. 10. Contact angles as a function of time for S-PANI DCX, S_PANI TCL and S-PANI GA membranes.

3.6.2. *Filtration in DMF of chemically cross-linked S-PANI membranes*

Visual studies have shown that chemically cross-linked S-PANI membranes have an improved solvent stability in harsh aprotic solvents. We further assessed this stability during filtration in DMF re-using the same membrane sample after 1 week. For this filtration study, we chose 7 months old membranes. Fig. 13 shows DMF permeance over time from two different runs of the chemically cross-linked membranes. During the first run, the permeate was only slightly coloured and the flux did not increase over the 2 h of the filtration. S-PANI GA, S-PANI TCL and S-PANI DCX showed a stable permeance of 6.1 L m^{-2} h^{-1} bar, 6.9 L m^2 h^{-1} bar and 8.4 L m^{-2} h^{-1} bar respectively. During the second run, the permeate did not change colour and interestingly all the membranes showed a lower permeance. S-PANI GA was 4.2 L m^{-2} h^{-1} bar^{-1} and S-

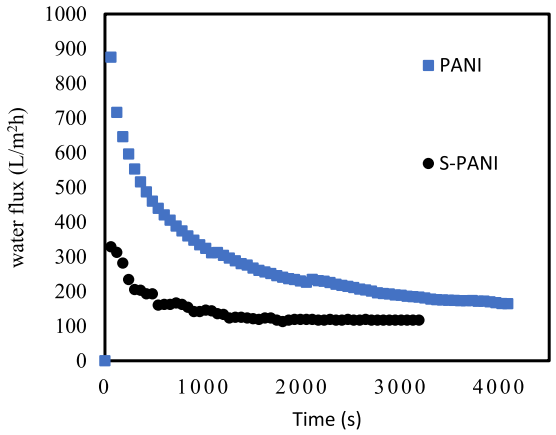

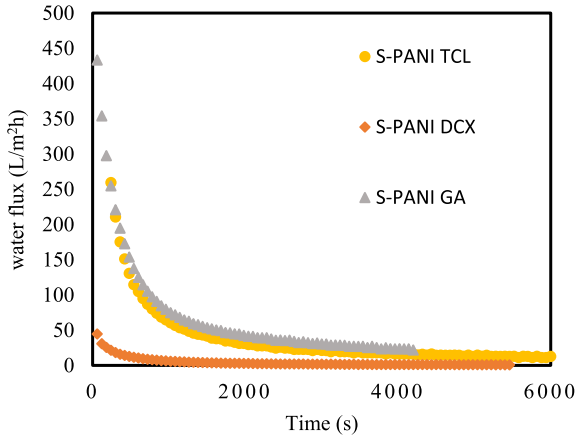

Fig. 11. Typical flux profile of initial period for filtration in dead-end cell. Operation conditions: 1 bar and 25 °C.

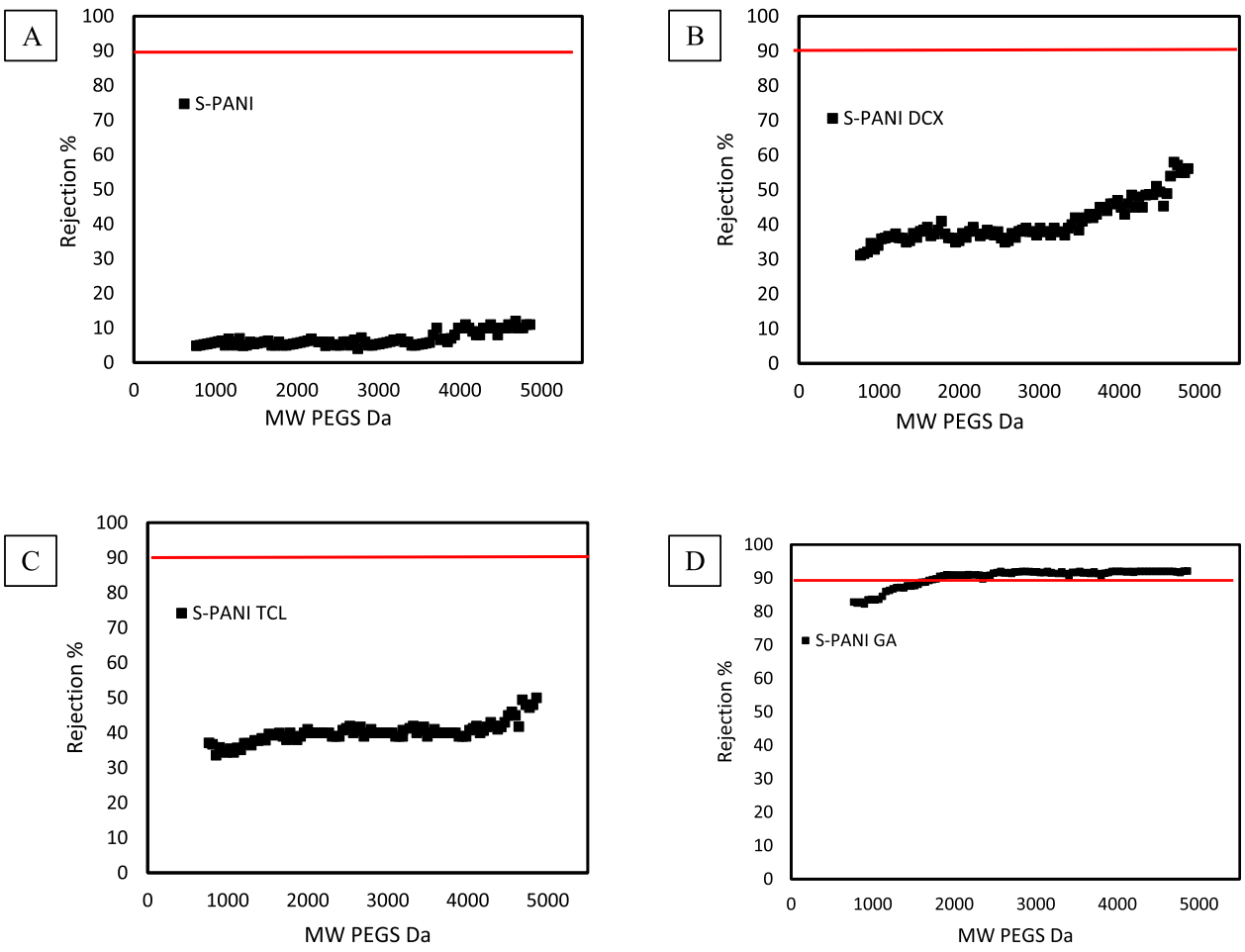

Fig. 12. Rejection curve of (A) S-PANI and chemically cross-linked S-PANI membranes: (B) S-PANI DCX, (C) S-PANI TCL and (D) S-PANI GA. Operation conditions are 1 bar, 25 °C, dead-end filtration.

PANI DCX was 4.8 L m^{-2} h^{-1} bar^{-1}. S-PANI TCL showed the lowest value of 0.6 L m^{-2} h^{-1} bar^{-1}. In summary, these results showed the excellent chemical resistance and stability of chemically cross-linked S-PANI membranes in DMF.

3.6.3. *BSA experiments and fouling behaviour*

As completion of our study, we tested the effect of the incorporation of the sulfonic group during synthesis on membrane potential antifouling ability using BSA as a model foulant in cross-flow. For long-term stability test in cross-flow, pure S-PANI, PANI and S-PANI GA (best chemically cross-linked S-PANI) membranes were selected.

Experiments were performed using one membrane and running pure water for 1 h (Jw). Then the membrane was fouled with 1 g/L of BSA solution and the flux decline was recorded for 1 h. The cleaning step was performed washing thoroughly the membrane with pure water for half an hour and the flux recovery was recorded (JwI). The fouling-cleaning cycle was repeated twice (Jw II and Jw III). Fig. 14 reports the time-dependent flux values of S-PANI, PANI and S-PANI GA membranes. Fouling indexes calculated for the first cleaning cycle are reported in Table 3. S-PANI showed excellent antifouling behaviour during the first cycle in cross-flow with an FRR of the 87 ± 7% which was more significant than the 40 ± 2% FFR of PANI. During the first cycle, S-PANI showed also low irreversible fouling IFR value of 13 ± 4% which was much lower than the IFR of 60 ± 4% of PANI. Usually, higher values of FRR and lower IFR describe a membrane with good antifouling properties [6]. S-PANI GA showed similar results with very low IFR (17 ± 5%) and RFR (16 ± 6%) and an FRR of 83 ± 2%.

Results from this experiment show that protein adsorption is significantly reduced at the S-PANI surface compared to PANI membrane. It has been reported that the zwitterionic surface formed a hydration layer which stops the BSA absorption [6]. Both S-PANI and S-PANI GA membranes performed better during the first cycle showing a TFR of 39 ± 2 and 33 ± 6%, in contrast with PANI, which presented a very poor flux recovery and a high TFR% of 61 ± 5%. Overall after 3 continuous fouling and cleaning cycles S-PANI shows Fr of 60% starting from an initial flux value of 107 ± 2 l/m^2h, PANI shows Fr of 41% starting from 84 ± 2 l/m^2h and S-PANI GA showed Fr of 50% with initial flux of 14 ± 3 l/m^2h. Overall the performance of the PANI membranes improved after sulfonic groups were introduced demonstrating that S-PANI membranes can be of potential use as low-fouling membranes in UF processes without the need for additional treatments or complex preparation. Besides, the tested chemical cross-linked S-PANI membrane showed a good antifouling performance demonstrating that S-PANI could be used as low fouling polymer to fabricate solvent resistant tight UF membranes.

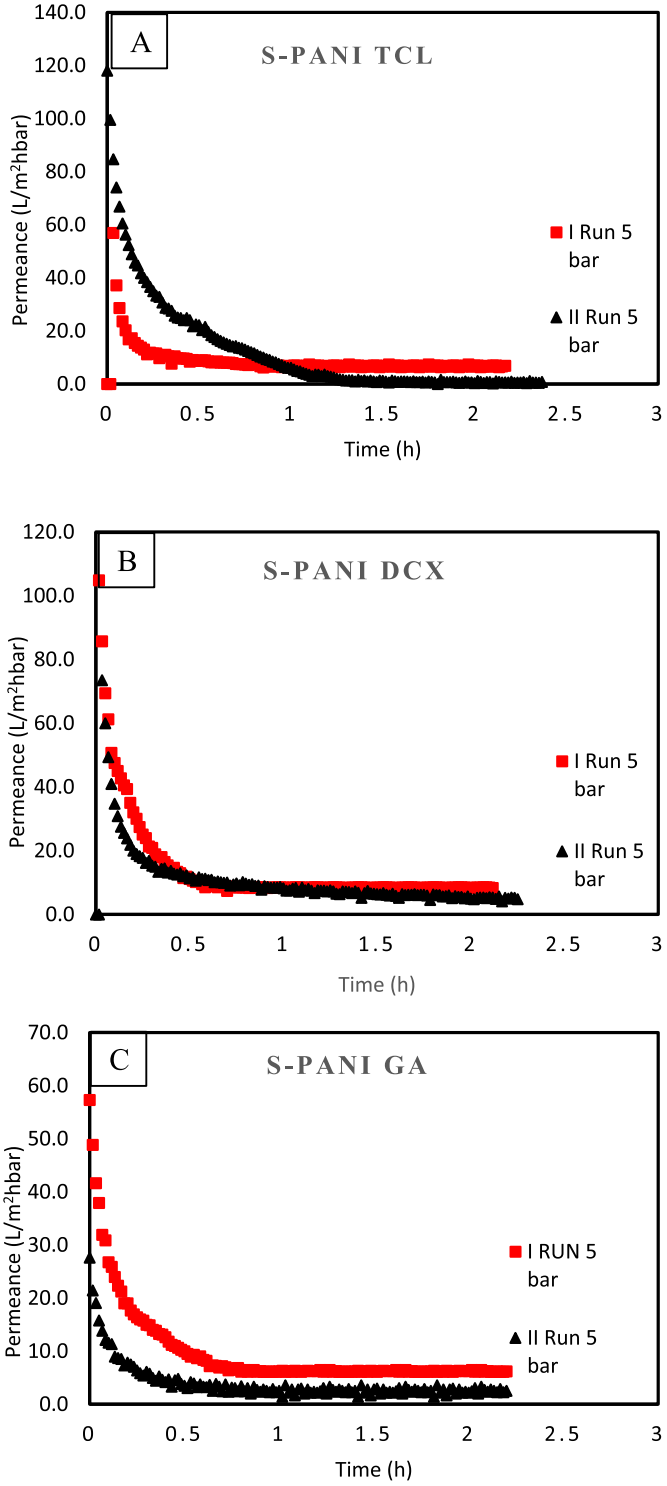

Fig. 13. DMF permeance over time of (A) S-PANI TCL, (B) S-PANI DCX, (C) S-PANI GA. Operation conditions are 5 bar, 25 °C, dead-end filtrations. The same membrane sample was used twice.

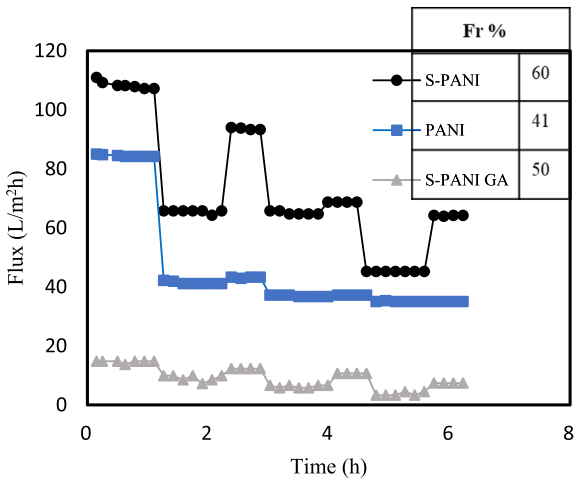

Fig. 14. Time dependent flux of S-PANI, PANI and S-PANI GA membranes tested in cross-flow with BSA.

Table 3
Fouling indexes for S-PANI and PANI membranes related to the first cleaning-fouling cycle.

	FRR %	TFR %	RFR %	IFR %
PANI	40 ± 3	61 ± 5	2 ± 1	60 ± 4
S-PANI	87 ± 7	39 ± 2	25 ± 4	13 ± 4
S-PANI GA	83 ± 2	33 ± 6	16 ± 6	17 ± 5

4. Conclusions

We have demonstrated the first fabrication and characterisation of S-PANI and chemically cross-linked S-PANI membranes. The membranes were synthesised from S-PANI powder and prepared through non-solvent phase inversion and their subsequent modification with organic cross-linkers. Pure S-PANI membrane showed similar morphology, flux, rejection and operating pressure as PANI. Chemical cross-linking successfully yielded long-term solvent (DMF) stable membranes with excellent reusability, improved PEG-rejection and ability to operate at high pressure (20 bar), showing the potential of chemically cross-linked S-PANI membranes. The flux recovery ratio and other flow indices showed significant improvement of fouling resistance of the S-PANI and S-PANI GA membranes compared to PANI membranes. The chemical cross-linking did not negatively affect the fouling resistance despite the slight increase of contact angle. This demonstrates that robust and durable hydrophilic low fouling S-PANI membranes can successfully be prepared using a versatile method that avoids dedoping of S-PANI powder with ammonium hydroxide and any other post-treatment. Furthermore, chemical cross-linking can further improve the solvent resistance whilst retaining low fouling properties. These newly developed S-PANI membranes with excellent solvent stability and fouling resistance, have strong potential to favorably extend the lifetime of membrane processes and reduce the operational costs and frequent chemical cleaning.

Declaration of competing interest

The authors declare that they have no known competing financial interests or personal relationships that could have appeared to influence the work reported in this paper.

Acknowledgements

The authors acknowledge the financial support of the European Research Council (ERC) Consolidator grant TUNEMEM (Project reference: 646769; funded under H2020-EU.1.1.-EXCELLENT SCIENCE)

Appendix A. Supplementary data

Supplementary data to this article can be found online at https://doi.org/10.1016/j.memsci.2019.117712.

References

[1] B.S. Lalia, V. Kochkodan, R. Hashaikeh, N. Hilal, A review on membrane fabrication: structure, properties and performance relationship, Desalination 326 (2013) 77–95.

[2] W. Guo, H.-H. Ngo, J. Li, A mini-review on membrane fouling, Bioresour. Technol. 122 (2012) 27–34.

[3] D. Rana, T. Matsuura, Surface modifications for antifouling membranes, Chem. Rev. 110 (2010) 2448–2471.

[4] S. Kiani, S.M. Mousavi, E. Saljoughi, N. Shahtahmassebi, Preparation and Characterization of Modified Polyphenylsulfone Membranes with Hydrophilic Property for Filtration of Aqueous Media, Polymers for Advanced Technologies, 2018.

[5] B.T. McVerry, J.A.T. Temple, X. Huang, K.L. Marsh, E.M.V. Hoek, R.B. Kaner, Fabrication of low-fouling ultrafiltration membranes using a hydrophilic, self-doping polyaniline additive, Chem. Mater. 25 (2013) 3597–3602.

[6] G. Rong, D. Zhou, J. Pang, Preparation of high-performance antifouling polyphenylsulfone ultrafiltration membrane by the addition of sulfonated polyaniline, J. Polym. Res. 25 (2018) 66.

[7] P.-F. Ren, Y. Fang, L.-S. Wan, X.-Y. Ye, Z.-K. Xu, Surface modification of polypropylene microfiltration membrane by grafting poly(sulfobetaine methacrylate) and poly(ethylene glycol): oxidative stability and antifouling capability, J. Membr. Sci. 492 (2015) 249–256.

[8] J. Ayyavoo, T.P.N. Nguyen, B.-M. Jun, I.-C. Kim, Y.-N. Kwon, Protection of polymeric membranes with antifouling surfacing via surface modifications, Colloid. Surf. Physicochem. Eng. Asp. 506 (2016) 190–201.

[9] A. Akbari, Z. Derikvandi, S.M. Mojallali Rostami, Influence of chitosan coating on the separation performance, morphology and anti-fouling properties of the polyamide nanofiltration membranes, J. Ind. Eng. Chem. 28 (2015) 268–276.

[10] N. Nady, M.C.R. Franssen, H. Zuilhof, M.S.M. Eldin, R. Boom, K. Schroën, Modification methods for poly(arylsulfone) membranes: a mini-review focusing on surface modification, Desalination 275 (2011) 1–9.

[11] X. Zhao, C. He, Efficient preparation of super antifouling PVDF ultrafiltration membrane with one step fabricated zwitterionic surface, ACS Appl. Mater. Interfaces 7 (2015) 17947–17953.

[12] S. Gahlot, H. Gupta, P.K. Jha, V. Kulshrestha, Enhanced electrochemical performance of stable SPES/SPANI composite polymer electrolyte membranes by enriched ionic nanochannels, ACS Omega 2 (2017) 5831–5839.

[13] M.R. Anderson, B.R. Mattes, H. Reiss, R.B. Kaner, Conjugated polymer films for gas separations, Science (1991) 1412–1415.

[14] L. Xu, S. Shahid, A.K. Holda, E.A.C. Emanuelsson, D.A. Patterson, Stimuli responsive conductive polyaniline membrane: in-filtration electrical tuneability of flux and MWCO, J. Membr. Sci. 552 (2018) 153–166.

[15] M. Sairam, X.X. Loh, K. Li, A. Bismarck, J.H.G. Steinke, A.G. Livingston, Nanoporous asymmetric polyaniline films for filtration of organic solvents, J. Membr. Sci. 330 (2009) 166–174.

[16] J. Yue, Z.H. Wang, K.R. Cromack, A.J. Epstein, A.G. MacDiarmid, Effect of sulfonic acid group on polyaniline backbone, J. Am. Chem. Soc. 113 (1991) 2665–2671.

[17] J. Yue, A.J. Epstein, XPS study of self-doped conducting polyaniline and parent systems, Macromolecules 24 (1991) 4441–4445.

[18] J. Yue, A.J. Epstein, Synthesis of self-doped conducting polyaniline, J. Am. Chem. Soc. 112 (1990) 2800–2801.

[19] C.-H. Yang, Y.-K. Chih, H.-E. Cheng, C.-H. Chen, Nanofibers of self-doped polyaniline, Polymer 46 (2005) 10688–10698.

[20] Y. Tao, J.X. Zhao, C.X. Wu, Polyacrylamide hydrogels with trapped sulfonated polyaniline, Eur. Polym. J. 41 (2005) 1342–1349.

[21] L. Shi, F. Zeng, X. Cheng, K.H. Lam, W. Wang, A. Wang, Z. Jin, F. Wu, Y. Yang, Enhanced performance of lithium-sulfur batteries with high sulfur loading utilizing ion selective MWCNT/SPANI modified separator, Chem. Eng. J. 334 (2018) 305–312.

[22] E.T. Vilela, R.d.C.S. Carvalho, S. Yotsumoto Neto, R.d.C.S. Luz, F.S. Damos, Exploiting charge/ions compensating processes in PANI/SPANI/reduced graphene oxide composite for development of a high sensitive H2O2 sensor, J. Electroanal. Chem. 752 (2015) 75–81.

[23] I. Mav, M. Žigon, A. Šebenik, J. Vohlidal, Sulfonated polyanilines prepared by copolymerization of 3-aminobenzenesulfonic acid and aniline: the effect of reaction conditions on polymer properties, J. Polym. Sci. A Polym. Chem. 38 (2000) 3390–3398.

[24] X.X. Loh, M. Sairam, A. Bismarck, J.H.G. Steinke, A.G. Livingston, K. Li, Crosslinked integrally skinned asymmetric polyaniline membranes for use in organic solvents, J. Membr. Sci. 326 (2009) 635–642.

[25] R. Rohani, M. Hyland, D. Patterson, A refined one-filtration method for aqueous based nanofiltration and ultrafiltration membrane molecular weight cut-off determination using polyethylene glycols, J. Membr. Sci. 382 (2011) 278–290.

[26] L. Xu, S. Shahid, J. Shen, E.A.C. Emanuelsson, D.A. Patterson, A wide range and high resolution one-filtration molecular weight cut-off method for aqueous based nanofiltration and ultrafiltration membranes, J. Membr. Sci. 525 (2017) 304–311.

[27] Y. Furukawa, F. Ueda, Y. Hyodo, I. Harada, T. Nakajima, T. Kawagoe, Vibrational spectra and structure of polyaniline, Macromolecules 21 (1988) 1297–1305.

[28] L. Zhu, M.T. Swihart, H. Lin, Tightening polybenzimidazole (PBI) nanostructure via chemical cross-linking for membrane H2/CO2 separation, J. Mater. Chem. 5 (2017) 19914–19923.

[29] S. Bhadra, D. Khastgir, Determination of crystal structure of polyaniline and substituted polyanilines through powder X-ray diffraction analysis, Polym. Test. 27 (2008) 851–857.

[30] Y. Wang, H.D. Tran, L. Liao, X. Duan, R.B. Kaner, Nanoscale morphology, dimensional control, and electrical properties of oligoanilines, J. Am. Chem. Soc. 132 (2010) 10365–10373.

[31] P. Srinivasa Rao, B. Smitha, S. Sridhar, A. Krishnaiah, Preparation and performance of poly(vinyl alcohol)/polyethyleneimine blend membranes for the dehydration of 1,4-dioxane by pervaporation: comparison with glutaraldehyde cross-linked membranes, Separ. Purif. Technol. 48 (2006) 244–254.

[32] Y. Ma, F. Shi, J. Ma, M. Wu, J. Zhang, C. Gao, Effect of PEG additive on the morphology and performance of polysulfone ultrafiltration membranes, Desalination 272 (2011) 51–58.

[33] T.-H. Young, L.-W. Chen, Pore formation mechanism of membranes from phase inversion process, Desalination 103 (1995) 233–247.

[34] J. Aburabie, A.-H. Emwas, K.-V. Peinemann, Silane-crosslinked asymmetric polythiosemicarbazide membranes for organic solvent nanofiltration, Macromol. Mater. Eng. 304 (2019) 1800551.

[35] M. de Souza Araki, C. de Morais Coutinho, L.A.G. Gonçalves, L.A. Viotto, Solvent permeability in commercial ultrafiltration polymeric membranes and evaluation of the structural and chemical stability towards hexane, Separ. Purif. Technol. 71 (2010) 13–21.

[36] K.M. Persson, V. Gekas, G. Trägårdh, Study of membrane compaction and its influence on ultrafiltration water permeability, J. Membr. Sci. 100 (1995) 155–162.

[37] L.L. Xu, S. Shahid, D.A. Patterson, E.A.C. Emanuelsson, Flexible electro-responsive in-situ polymer acid doped polyaniline membranes for permeation enhancement and membrane fouling removal, J. Membr. Sci. 578 (2019) 263–272.

[38] N. Cheng, Q. Yan, S. Liu, D. Zhao, Probing the intermolecular interactions of aromatic amides containing N-heterocycles and triptycene, CrystEngComm 16 (2014) 4265–4273.